

Research Paper

Anterior Visceral Endoderm SMAD4 Signaling Specifies Anterior Embryonic Patterning and Head Induction in Mice

Cuiling Li¹, Yi-Ping Li², Xin-Yuan Fu³, and Chu-Xia Deng¹ ✉

1. Mammalian Genetics Section, Genetics of Development and Disease Branch, National Institutes of Diabetes and Digestive and Kidney Diseases, National Institutes of Health, 10/9N105, 10 Center Drive, Bethesda, MD 20892, USA
2. Department of Cytokine Biology, The Forsyth Institute, Boston, MA 02115, USA
3. Department of Biochemistry, Yong Loo Lin School of Medicine, National University of Singapore, 8 Medical Drive, MD7 #02-03, Singapore 117597

✉ Corresponding author: Chu-Xia Deng, Phone: 301-402-7225; Fax: 301-480-1135; Email: chuxiad@bdg10.niddk.nih.gov

Received: 2010.09.16; Accepted: 2010.09.27; Published: 2010.09.27

Abstract

SMAD4 serves as a common mediator for signaling of TGF- β superfamily. Previous studies illustrated that SMAD4-null mice die at embryonic day 6.5 (E6.5) due to failure of mesoderm induction and extraembryonic defects; however, functions of SMAD4 in each germ layer remain elusive. To investigate this, we disrupted SMAD4 in the visceral endoderm and epiblast, respectively, using a Cre-loxP mediated approach. We showed that mutant embryos lack of SMAD4 in the visceral endoderm (*Smad4^{Col/Col};TTR-Cre*) died at E7.5-E9.5 without head-fold and anterior embryonic structures. We demonstrated that TGF- β regulates expression of several genes, such as *Hex1*, *Cer1*, and *Lim1*, in the anterior visceral endoderm (AVE), and the failure of anterior embryonic development in *Smad4^{Col/Col};TTR-Cre* embryos is accompanied by diminished expression of these genes. Consistent with this finding, SMAD4-deficient embryoid bodies showed impaired responsiveness to TGF- β -induced gene expression and morphological changes. On the other hand, embryos carrying Cre-loxP mediated disruption of SMAD4 in the epiblasts exhibited relatively normal mesoderm and head-fold induction although they all displayed profound patterning defects in the later stages of gastrulation. Cumulatively, our data indicate that SMAD4 signaling in the epiblasts is dispensable for mesoderm induction although it remains critical for head patterning, which is significantly different from SMAD4 signaling in the AVE, where it specifies anterior embryonic patterning and head induction.

Key words: TGF-beta, SMAD4, AVE, epiblast, mesoderm patterning

Introduction

Gastrulation is a process in which embryos form three layered structures known as the mesoderm, ectoderm and endoderm [1-3]. Signaling from different layers interact with each other to ensure normal embryonic patterning and differentiation [1-3]. Within these three layers exist many molecules, including members of TGF- β superfamily, their receptors and intracellular mediators that are important for initiation of gastrulation, head induction and patterning [3-11]. For example, embryos carrying a mutation of

TGF- β family members (such as BMP4 or Nodal), and their receptors (type I receptor ActRIB or the type II receptors ActRIIA/ActRIIB), either arrest at egg cylinder stages prior to mesoderm induction or die during gastrulation with severe patterning defects [12-15], highlighting an important function of TGF- β signaling in gastrulation and mesoderm induction. In light of these findings, it is important to point out that the precise role of each component of TGF- β signaling cascade in each of these distinct layers are often dif-

difficult to assess, as the conventional knockout approach disrupts genes in entire embryos.

SMAD proteins serve as a major intracellular component of TGF- β signaling pathway [7-9, 16]. There are eight members in the SMAD family where SMAD4 serve as a common mediator for TGF- β signaling. SMAD4 is a well-known tumor suppressor as its mutations have been detected in many human cancers, including pancreatic cancer, colon cancer, cholangiocarcinoma cancer, and gastric adenocarcinomas [17-19]. Mice carrying SMAD4 somatic mutations, generated by Cre-loxP approach to overcome embryonic lethality of germline mutation, develop cancers in the liver, pancreas, colon, skin, and many other organ/tissues [20-26]. To date, all SMADs have been knocked out in mice, and SMAD4-deficient mice exhibited the most severe phenotype than any other mice carrying targeted mutations of other SMADs (reviewed in [10, 27], which is consistent with its function as a common mediator for TGF- β signaling.

Smad4^{-/-} embryos died shortly after implantation at egg cylinder stages, exhibiting profound reduced cellular proliferation [28, 29]. Several lines of evidence indicated that the primary defect caused by SMAD4 deficiency is in the visceral endoderm. First, *Smad4*^{-/-} embryos exhibited more severe abnormalities in the extraembryonic tissues than embryonic portion [29]. Second, *Smad4*^{-/-} ES cells failed to make a normal visceral endoderm in embryoid body differentiated *in vitro* [28]. Third, embryos that carried a Cre-LoxP mediated deletion of SMAD4 in the epiblast but not in the visceral endoderm formed many mesodermal derivatives, including somites, heart, allantois and lateral plate mesoderm [30], suggesting the absence of SMAD4 in the epiblast does not block mesoderm formation.

Therefore, we hypothesized that SMAD4 signaling in visceral endoderm specify mesoderm formation. To test this hypothesis, we performed a tissue specific disruption of SMAD4 in the visceral endoderm. Our analysis indicated that SMAD4 mutant embryos failed to express a number of key molecules in the AVE and were arrested at E7.5-E8.5 lacking head and anterior embryonic structures. Our data reveals an essential role of SMAD4 in the visceral endoderm in anterior embryonic patterning and head induction during gastrulation.

Results

Expression of *TTR-Cre*

Transgenic mice carrying a *Cre* gene controlled by transthyretin (*TTR*) promoter was used to delete

SMAD4. Using a Rosa-26 reporter strain (R26R) for Cre activity [31], *TTR-Cre* mediated recombination was detected in embryonic (E) 5.75 embryos at both embryonic and extraembryonic endoderm (Fig. 1A). The cells carrying *TTR-Cre* mediated recombination (β -gal positive) gradually spread into the entire endoderm of the embryos at E6-6.5 (Fig. 1B, C, D). As the mesoendoderm gradually replaces the distal endoderm, visceral endoderm gradually retreats toward extraembryonic portion. By E7.5, the β -gal positive cells were restricted to the visceral endoderm mainly at the extraembryonic portion (Fig. 1E, F). At E8.5, Cre-mediated recombination is detected in the embryo starting from the primitive endoderm near the caudal neuropore (the tip of the hindgut) (Fig. 1G). At E9.5, the β -gal⁺ cells spreads to most part of the gut epithelium (arrows, Fig. 1H, I), and they also populated the endoderm-derived layer (the out layer) of the yolk sac (Fig. 1I).

Severe gastrulation defects in mice carrying a targeted deletion of SMAD4 in the visceral endoderm

Visceral endoderm specific deletion of SMAD4 is achieved by crossing SMAD4 conditional mutant mice [32] with *TTR-Cre* transgenic mice. The *Smad4*^{+/Co};*TTR-Cre* mice were normal and were further crossed with *Smad4*^{Co/Co} mice to generate *Smad4*^{Co/Co};*TTR-Cre* embryos. Our analysis on 41 offspring generated by this cross failed to obtain any *Smad4*^{Co/Co};*TTR-Cre* mice at post-neonatal stages, indicating that they were embryonic lethal (Table 1). Upon closer examination we determined that *Smad4*^{Co/Co};*TTR-Cre* embryos died before E9.5 (Table 1). Our data indicated that the mutant embryos were slightly smaller at E6.5 but became smaller at E7.5 (Fig. 2A) and at E8.5-9.5, the embryonic portion of mutant embryo was significantly smaller and maintained as a solid mass sticking out of the yolk sac (Fig. 2B-D). There was a correlation between the age of the embryos and their size. As they increased in age, their size significantly decreased. Upon histological examination, the *Smad4*^{Co/Co};*TTR-Cre* embryos were disorganized, lacking anterior and middle trunk structures (Fig. 2E-H). They had enlarged allantois and some visible, yet abnormal posterior structures (Fig. 2E-H). Cross section revealed the existence of neural epithelium although it was also quite abnormal (Fig. 2I,J). Together, the data indicate that the absence of SMAD4 does not block mesoderm induction; however, it causes severe defects during gastrulation.

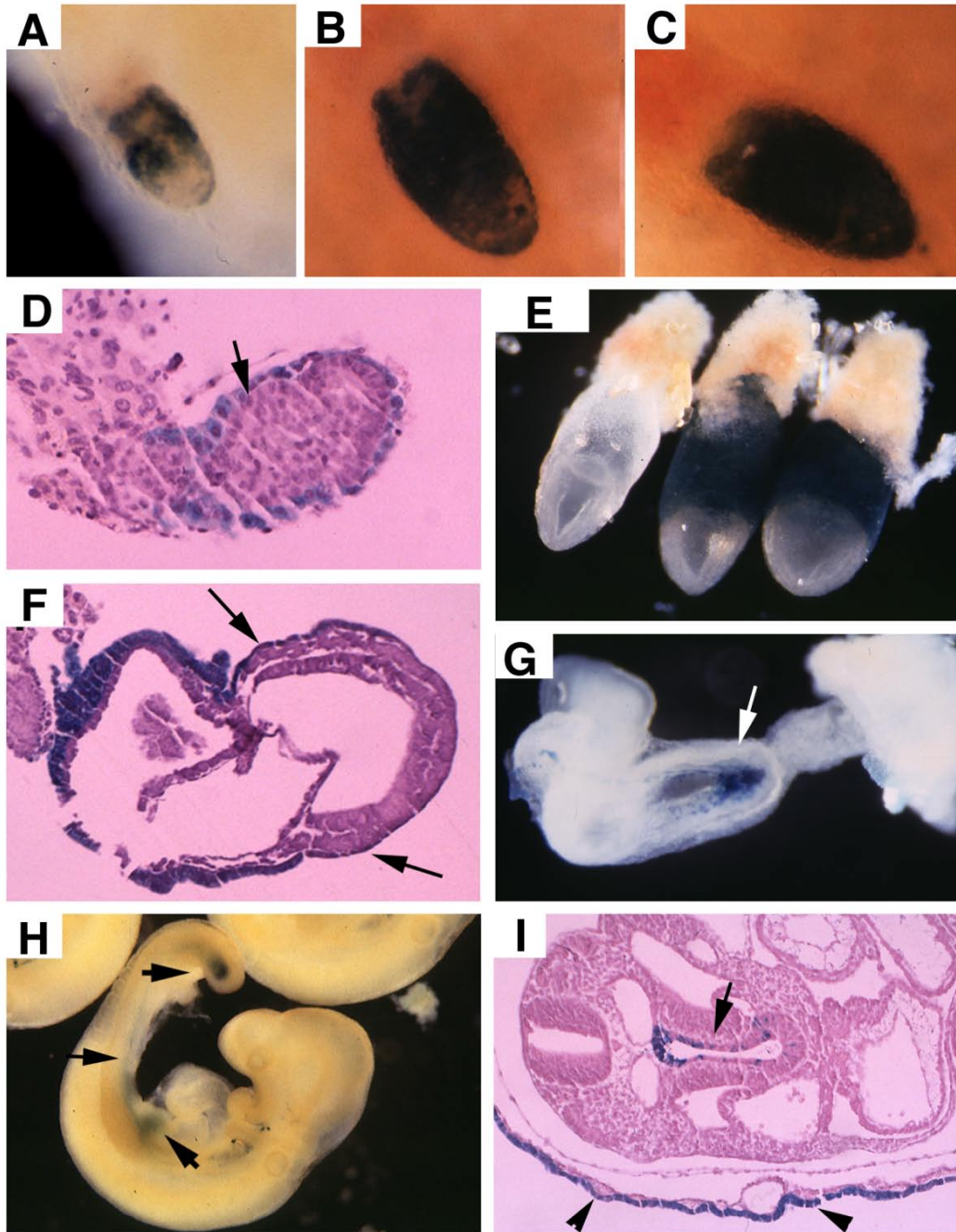


Fig. 1. TTR-Cre activity in early post-implantation embryos. (A-D), Images of *Rosa-R26R;TTR-Cre* embryos at E5.75-E6.5 revealed by X-Gal staining. (E,F) X-Gal staining in extraembryonic endoderm of two E7.5 *Rosa-R26R;TTR-Cre* embryos (right in E). Arrows point to weak X-Gal staining in visceral endoderm portion that covers the epiblast, which will development into the visceral yolk sac later (F). (G) At E8.5, *TTR-Cre* is expressed in the primitive endoderm near the caudal neuropore (arrows). (H,I) At E9.5, it expressed in tail bud and some tissues derived from midgut endoderm (arrows in H), and also in the visceral yolk sac (arrowhead in I, arrow points to gut epithelium). At least 10 embryos at each time point were analyzed for the staining.

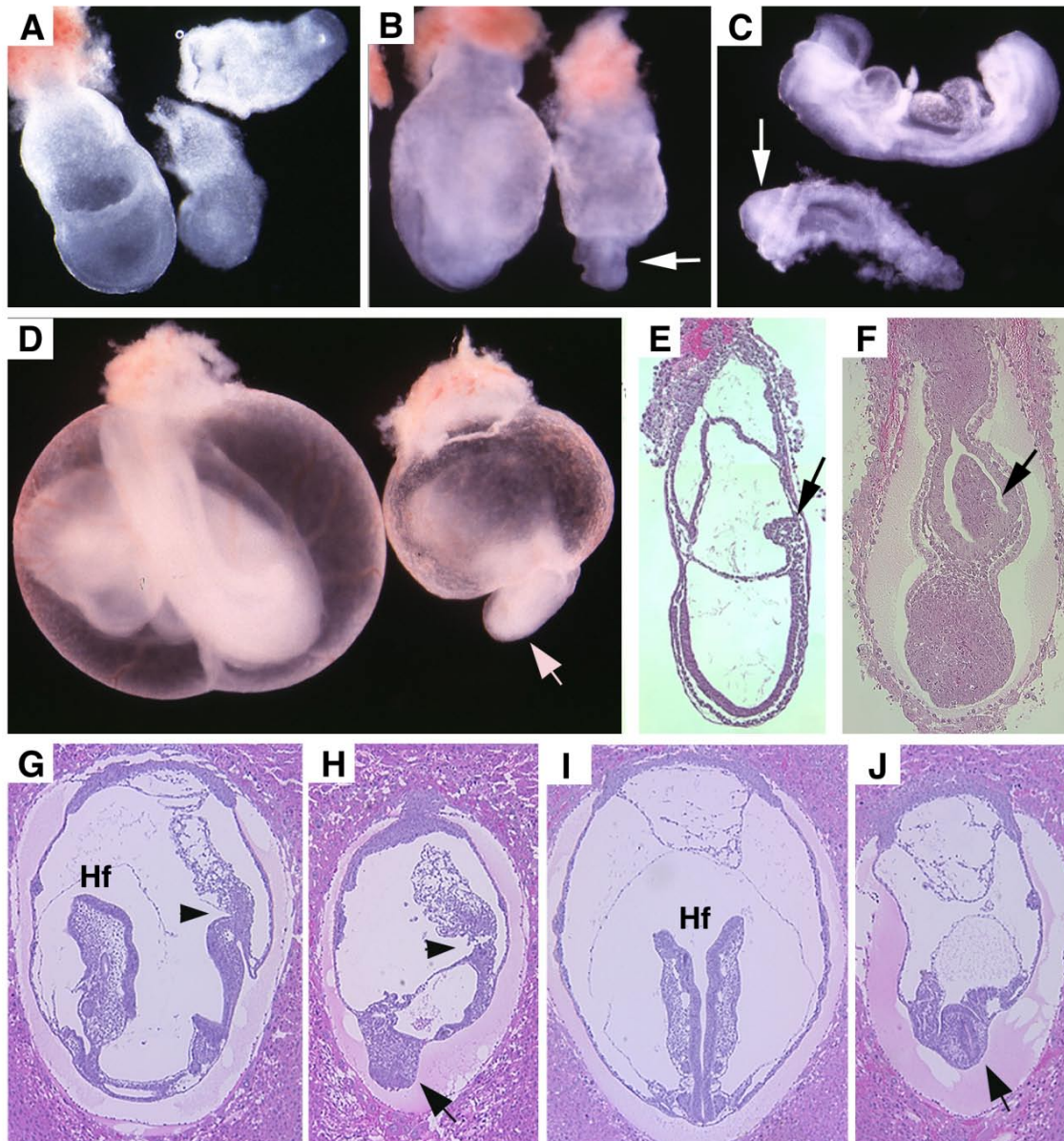


Fig. 2. Morphology and histology of *Smad4^{ColCo};TTR-Cre* embryos. (A-D) Morphology of E7.5 (A) E8.5 (B,C) and E9.5 (D) embryos. *Smad4^{ColCo};TTR-Cre* mutant embryos were pointed by arrows. Anterior region protrudes out from yolk sac in the *Smad4^{ColCo};TTR-Cre* mutant embryos (arrows in B-D). (E-J) Histology of E7.5 (E,F) and E8.5 (G-J) control embryos (E,G,I) and *Smad4^{ColCo};TTR-Cre* mutant embryos (F,H,J). Arrows in E,F, and arrowhead in G,H point allantois. Arrows in H,J point to anterior truncation in the mutant embryos presented at different angles. Hf: head-fold. At least 4 *Smad4^{ColCo};TTR-Cre* mutant embryos at each time point were analyzed.

Table 1. Genotypes and phenotypes of offspring from crosses between *Smad4^{Co/Co}* and *Smad4^{Co/+};TTR-Cre* mice^a

	Total	Co/Co	Co	Co/+;Cre	Co/Co;Cre ^b	resorption
Neonates	41	12	15	14	0	0
E16.5	7	3	1	3	0	0
E13.5	9	1	4	3	0	1
E12.5-16.5	11	1	4	1	0	5
E10.5	30	5	7	10	3	5
E9.5	17	4	4	2	7	0
E8.5	9	2	2	2	3	0
E7.5	25	7	4	8	6	0
E6.5	16	2	4	6	4	0

a. The cross between *Smad4^{Co/Co}* and *Smad4^{Co/+};TTR-Cre* should yield equal number of offspring with each of four different genotypes if they are not lethal. However, there are no live *Smad4^{Co/Co};TTR-Cre* mice and *Smad4^{Co/Co};TTR-Cre* embryos were under represented starting from E10.5.

b. All *Smad4^{Co/Co};TTR-Cre* embryos are abnormal

Loss of SMAD4 impairs AVE signaling and causes truncation of anterior and middle trunk of gastrulating embryos

Next, we studied markers for AVE signaling as it plays a critical role in specifying head formation and anterior mesoderm patterning in mouse embryos [6, 33, 34]. At E6, *Cer1*, which marks the AVE and the earliest population of anterior definite endoderm [35] is detected in the AVE of wild-type embryos, and maintained distinct expression levels throughout E7.5 (Fig. 3A-C). However, *Cer1* was significantly reduced or absent in SMAD4 mutant embryos at all the time points examined (Fig. 3A'-C'). Next, we examined *Lim1*, which is expressed in the AVE and also in a region of the epiblast where the future primitive streak forms prior to gastrulation [36]. At early gastrulation, *Lim1* is present in the primitive streak, migrating mesodermal wings and the prechordal mesoderm that underlies the anterior portion of the future head-fold (Fig. 3D). In the SMAD4 mutant embryos, expression of *Lim1* was significantly decreased in the posterior region and was diminished in the AVE (Fig. 3D'). We also observed similar reduced expression of *Hnf3 β* (data not shown). Despite these changes, SMAD4 mutant embryos were able to initiate gastrulation as evidenced by expression of *T* gene in the primitive streak although the development is much delayed and the primitive streak is much shorter compared with the control embryos (Fig. 3E,E'). Histological sections prepared at different angles of embryos at E6.5 (Fig. 3F,F') and E7.5 (Fig.

3G,G') revealed abnormal accumulations of cells in the mutant embryos.

Abnormal head-fold formation was further analyzed using molecular markers.

Otx2 is expressed in the epiblast prior to gastrulation in the wild-type embryos (Fig. 4A). No significant difference of *Otx2* was observed in mutant embryos although they were smaller than controls at this stage (Fig. 4B). During gastrulation, *Otx2* expressing cells progressively restricted to anterior portion of the embryo, and demarcated the anterior neuroectoderm in normal embryos (Fig. 4C,D). In the mutant embryos, the *Otx2* expression domain was much smaller and presented in the poorly developed distal portion of the embryos (Fig. 4C,D). At E9.5 *Otx2* expression marked the forebrain and midbrain (Fig. 4E), however, it disappeared in the mutant embryos (Fig. 4F).

Next, we examined the development of the midbrain and hindbrain of SMAD4 mutant embryos. Staining of a midbrain marker, *En-1*, detected the existence of some residue cells in the midbrain (Fig. 4F). Mutant embryos also maintained a narrow stripe of rhombomere 5 revealed by using *Krox20*, which marks rhombomeres 3 and 5 (Fig. 4G). Staining of *Mox1*, a marker for somites (Fig. 4H,I), and *Lim1*, which marks areas in the urogenital precursor (Fig. 4J), revealed relative normal posterior structures. These data indicate that targeted disruption of SMAD4 in visceral endoderm resulted in a failure to establish the anterior-posterior (A-P) axis characterized by truncation of anterior and middle trunk of gastrulating embryos.

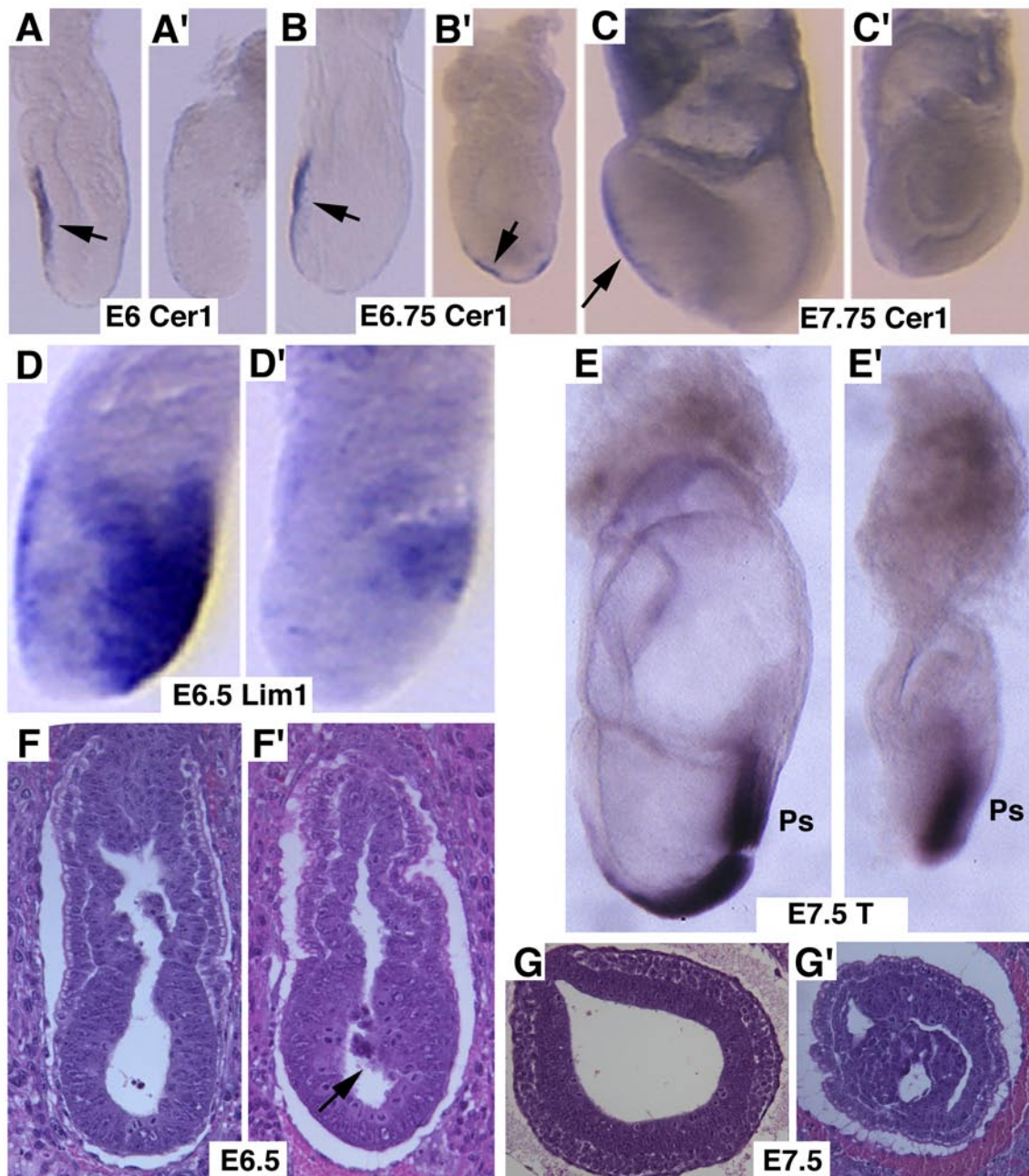


Fig. 3. Marker analysis of *Smad4*^{Col/Col};*TTR-Cre* embryos at E6-7.5. (A-C) *Cer1* expression is dramatically reduced in the *Smad4*^{Col/Col};*TTR-Cre* embryos (A', B', C') compared with controls (A-C). (D) *Lim1* expression level is reduced in the posterior region and missing in the AVE of the mutant embryos (D'). (E) Expression of *T*, which marks the primitive streak (ps), is detected at both E7.5 control (E) and mutant (E') embryos, however the ps is much shorter in the mutant embryo. (F,G) Sagittal (F) and cross (G) sections of embryos showing accumulation of cells (arrow in F') and abnormally positioned cells (G') in the mutant embryos. At least 6 *Smad4*^{Col/Col};*TTR-Cre* embryos were analyzed for each marker at each time point.

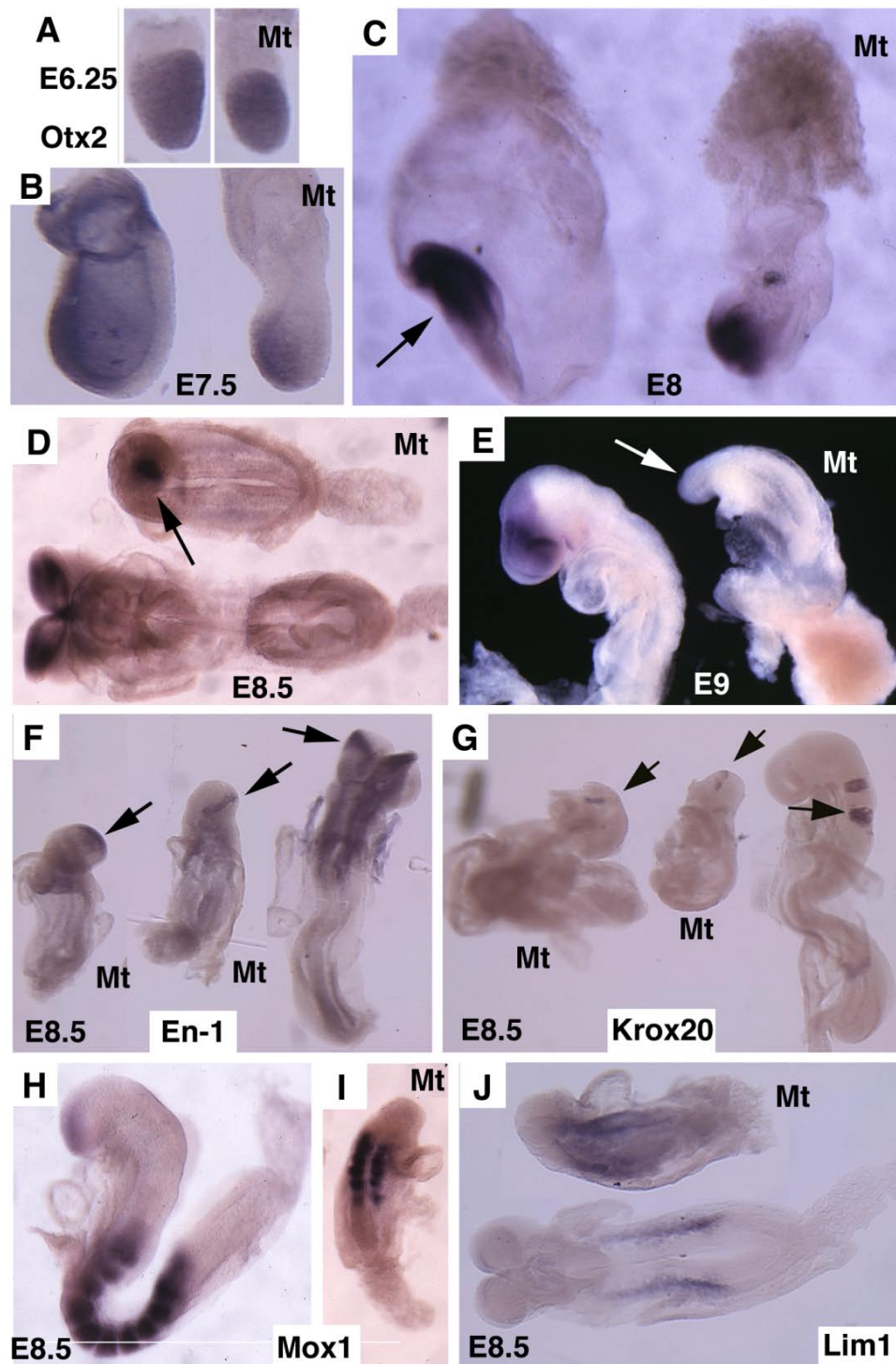


Fig. 4. Molecular marker analysis for *Smad4^{ColCo};TTR-Cre* embryos. (A-E) Expression of Otx2 in control and mutant (Mt) embryos at different stages as indicated. Arrow in C points to the headfold of a control embryo. Arrows in D,E point to anterior of mutant embryos. (F-J) Expression of En1 (F), Krox20 (G), Mox1 (H,I) and Lim1 (J). Arrows in F,G, point to expression of Krox20 (F) and En1 (G). At least 4 *Smad4^{ColCo};TTR-Cre* embryos were analyzed for each marker at each time point.

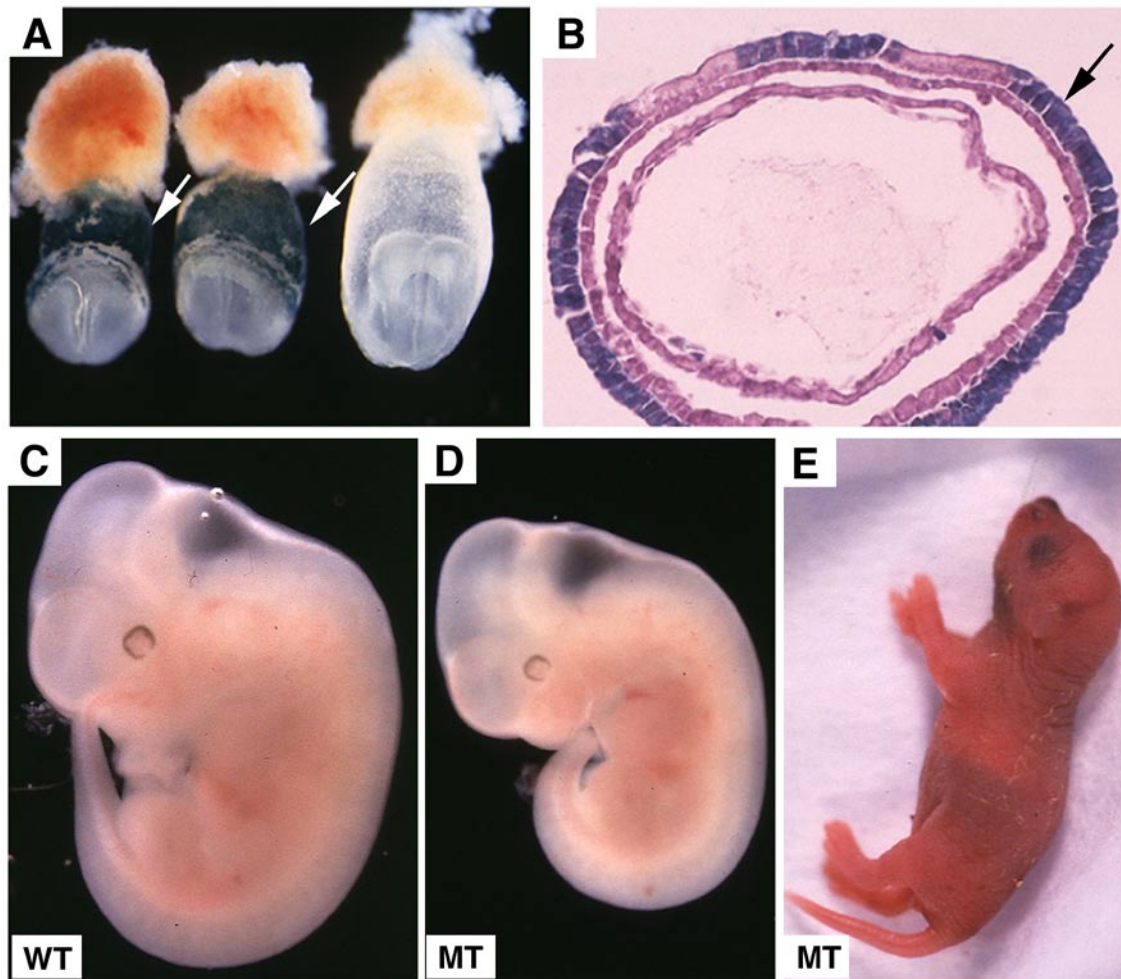


Fig. 5. Embryonic lethality of *Smad4*^{Col/Col};*TTR-Cre* embryos was rescued by fusion with wild type tetraploid embryos. (A,B) Contribution of tetraploid cells to extraembryonic tissues analyzed at E7.5 embryos by wholemount view (A) and histological sections (B). Arrows point tetraploid beta-gal positive cells that are generated from embryos of Rosa-26 mice after fusion. (C,D) Tetraploid embryos fused wild type (C) and *Smad4*^{Col/Col};*TTR-Cre* (D) embryos at E11.5. (E) A rescued *Smad4*^{Col/Col};*TTR-Cre* mutant mouse at birth.

Wild-type tetraploid extraembryonic tissue rescues the lethality of *Smad4*^{Col/Col};*TTR-Cre* embryos

Tetraploid cells are known to preferentially contribute to extraembryonic tissues as demonstrated previously [37, 38] and in this study (Fig. 5A,B). To confirm that the lethality of *Smad4*^{Col/Col};*TTR-Cre* embryos is indeed caused by the deletion of SMAD4 in the extraembryonic endoderm, we aggregated *Smad4*^{Col/Col};*TTR-Cre* embryos with wild-type tetraploid embryos. In the three litters of embryos analyzed at E10.5-11.5, we found 5 morphologically normal *Smad4*^{Col/Col};*TTR-Cre* embryos (Fig. 5C,D) and one partially rescued SMAD4 mutant embryo (data not shown). Because we never observed any

Smad4^{Col/Col};*TTR-Cre* embryos without fusing with tetraploid embryos that displayed normal or nearly normal morphology at these stages (Table 1), We concluded that wild-type tetraploid extraembryonic tissue repressed the lethality of *Smad4*^{Col/Col};*TTR-Cre* embryos and allowed them to develop through gastrulation. Some of them even advanced to birth (Fig. 5E). This observation provides strong evidence that extraembryonic tissue is critical for early post-implantation embryogenesis and normal patterning.

Deletion of SMAD4 in the epiblast yields less severe phenotypes than its deletion in the visceral endoderm

Previous investigations generated SMAD4 mu-

tant embryos with wild-type endoderm either using wild-type tetraploid embryos to fuse with SMAD4^{-/-} embryos [28] or knocking out SMAD4 in the epiblast specifically using *Sox2-Cre* [30]. Their data revealed that that wild-type visceral endoderm could rescue the gastrulation defect of *Smad4*-deficient embryos. To provide first hand comparative information regarding a role of SMAD4 in different germ layers during early embryonic development, we interbred the *Smad4*^{Co/Co} mice with *Mox2-Cre* mice, which also specifically express Cre in the epiblast [39](Fig. 6A,B) but at a stage that slightly late than *Sox2-Cre* [40]. Our analysis indicated that the *Smad4*^{Co/Co};*Mox2-Cre* embryos were slightly smaller than control embryos in the early stages of gastrulation (Fig. 6C). Most *Smad4*^{Co/Co};*Mox2-Cre* embryos maintained relatively normal *Lim1* (Fig. 6C) and *Cer1* (Fig. 6D) expression. The mutant embryos were able to initiate gastrulation as revealed by the formation of the primitive streak although in most cases the mutant primitive streak is shorter (Fig. 6E). All mutant embryos advanced to the head-fold stage as revealed by *Otx2* expression (Fig. 6F) and the morphological appearance at E7.75-E8.75 despite the fact that they were clearly abnormal at these stages (Fig. 6G-I). Further analysis using whole-mount in situ hybridization with lineage markers revealed that *Smad4*^{Co/Co};*Mox2-Cre* embryos formed notochord as revealed by sonic hedgehog (*Shh*, Fig. 6J), and forehead as revealed by brain factor (*Bfl*) (arrows, Fig. 6K,L). Of note, they also displayed expanded left-right (L-R) axis as revealed by paraxial mesoderm marker, *Mox1*, compared with controls (Fig. 6M). Hybridization with *Lim1* for developing mesonephros in the middle trunk of the embryos (arrowheads, Fig. 6K,L) and *HoxB9* for posterior neural ectoderm (Fig. 6N,L) detected slightly shortened posterior structures. Thus, despite the observation that *Smad4*^{Co/Co};*Mox2-Cre* embryos exhibited many patterning and morphogenesis defects, the absence of SMAD4 in the epiblast does not block anterior mesoderm formation and head-fold induction. The *Smad4*^{Co/Co};*Mox2-Cre* embryos also survived, on the average, one day longer than *Smad4*^{Co/Co};*TTR-Cre* embryos. These data suggest that SMAD4 plays a more critical role in the visceral endoderm than it does in the epiblast.

Absence of SMAD4 lost responsiveness to TGF- β induced morphogenetic changes and visceral endoderm gene expression in embryoid bodies

Embryoid bodies serve as an excellent model for

studying developmental signaling and early embryonic development. Therefore, we studied the response of embryoid body differentiation to TGF- β signaling. Upon TGF- β treatment, embryoid body underwent faster differentiation (Fig. 7A) compared with untreated controls (Fig. 7A'). We also detected up-regulation of VE marker genes, such as *Hex1* (Fig. 7B), *Cer1* (Fig. 7C), and *Lim1* (Fig. 7D) in the TGF- β treated samples compared with controls (Fig. 7B', C', D'). We next isolated RNA from both TGF- β treated and untreated embryoid bodies at different time points and analyzed gene expression (Fig. 7E). We found that *Lim1* level increased 24 hours upon TGF- β treatment. *EndoA*, also called mouse keratin 8 that serves as an endodermal marker for early embryos [41], was initially expressed at relatively higher levels and its expression became weaker during later days of differentiation in the untreated embryos. Treatment of TGF- β maintained higher expression levels at all time points examined, consistent with a role of TGF- β signaling in induction and maintaining endoderm cell fate. Expression of other two later endoderm marker genes, *Gata4* [42] and *Hnf1* [43] was induced 2 days after treatment. Meanwhile, expression of *T* gene, a marker for mesoderm, was induced 6 days after treatment. Collectively, the data indicate that morphogenetic change induced by TGF- β treatment is associated with distinct expression changes of genes involved in early embryonic development and germ layer formation.

To investigate whether this action of TGF- β is mediated by SMAD4, we treated embryoid bodies formed by SMAD4^{-/-} and wild-type ES cells with TGF- β . Our data indicated while TGF- β treatment readily up-regulated expression of genes involved in egg cylinder development (*Lim1* and *Hex1*) and endoderm formation (*Endo A* and *Hnf1*), SMAD4 mutant embryoid bodies showed impaired response or responsiveness to the treatment (Fig. 7F). Expression of *Nodal* is first detected in primitive streak-stage embryos at about the time of mesoderm formation, and then becomes highly localized in the node at the anterior of the primitive streak [15]. Consistent with late appearance of *T* expression (Fig. 7E), we detected weak expression of *Nodal* in E6 embryoid bodies, but its expression was not detected in SMAD4^{-/-} ES cells (Fig. 7F). These data provide strong evidence that SMAD4 mediates TGF- β signaling which in turn regulates expression of genes during early embryonic development and endoderm differentiation.

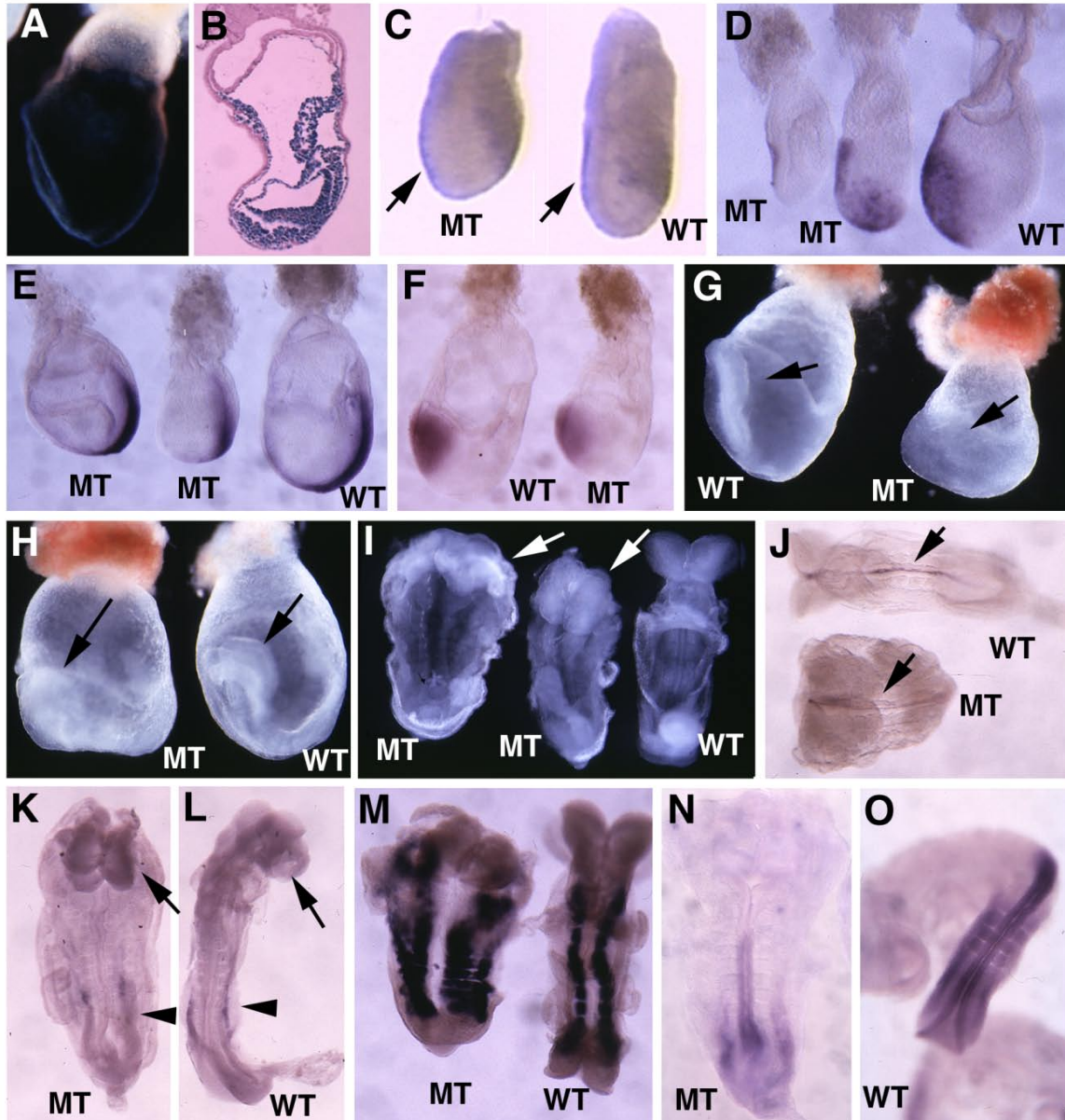


Fig. 6. Analysis for *Smad4^{Col/Col};Mox2-Cre* embryos.** (A,B) Images of *Rosa-R26R;**Mox2-Cre* embryos at E7.5 revealed by X-Gal staining. (C). Wholemount in situ hybridization with *Lim1* in E6.5 mutant (MT) and control (WT) embryos. (D-F) Expression of *Cer1* (D), *T* (E) and *Otx2* (F) in E7.5 embryos. (G,H) Morphological of E7.75 (G) and E8.5 (H) embryos before dissecting out from yolk sac. Arrow point to head-fold. (I) E8.5 embryos after dissecting out from yolk sac. (J-O) Expression of *SSH* (J), *BFI* (arrows in K,L), *Lim1* (arrowheads, in K,L), and *Mox1* (M) in E8.75 embryos, as well as *HoxB9* (N,O) in E9 embryos. At least 4-10 *Smad4^{Col/Col};**Mox2-Cre* embryos were analyzed for each marker at each time point.

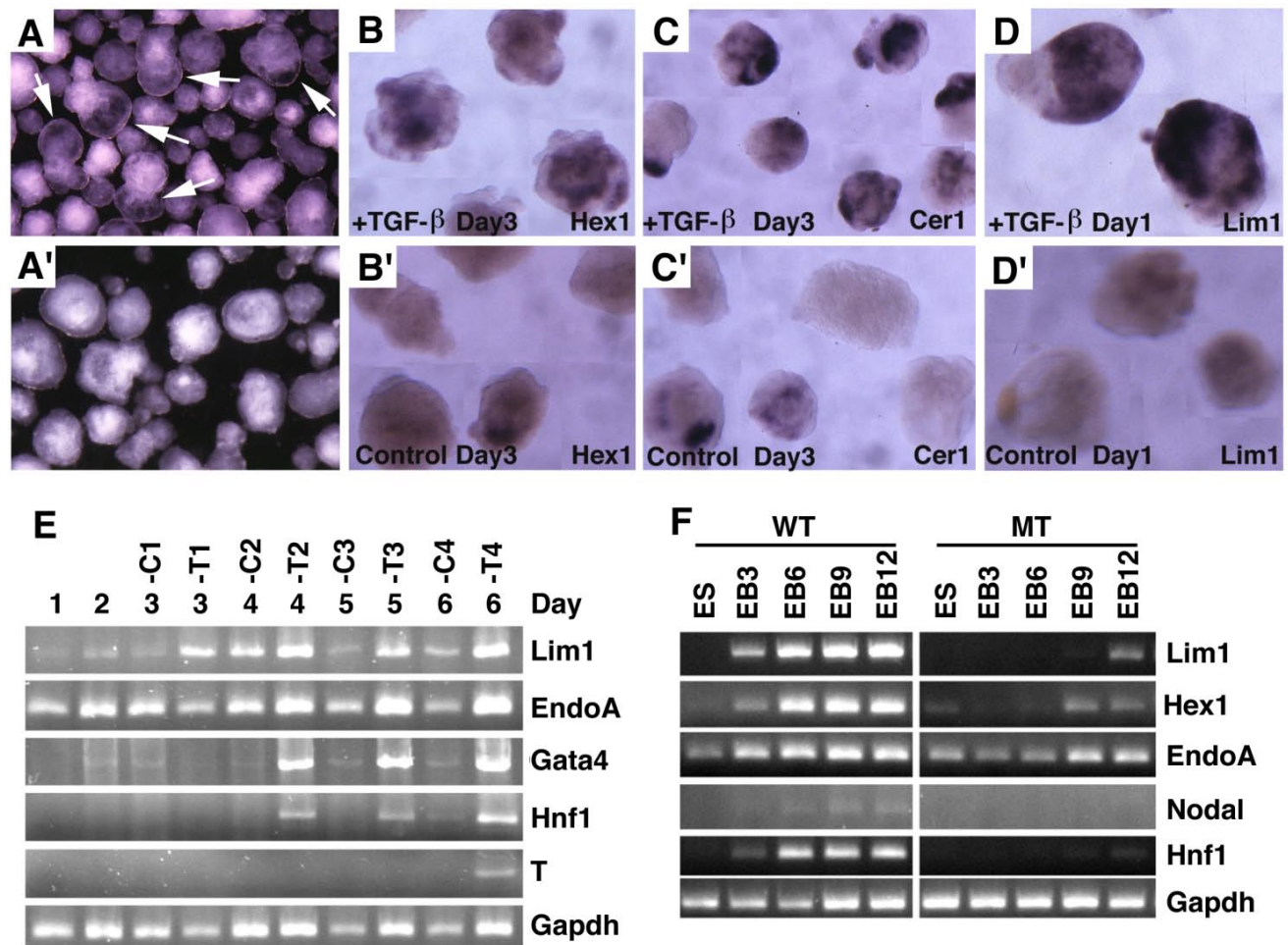


Fig. 7. Embryoid body culture and expression analysis of molecular markers. (A) Morphology of embryoid bodies that have been treated (A) or untreated (A') with TGF- β 1 (10ng/ml) for 4 days. Arrows in A point to cavities induced by TGF- β 1. (B-D) Gene expression of in TGF- β 1 treated (B-D) or untreated (B'-D') embryoid bodies revealed by wholemount in situ hybridization. (E). RT-PCR analysis of gene expression. RNA was isolated at different time points from both TGF- β 1 treated (T) and untreated (C) embryoid bodies. TGF- β 1 was added 48 hours after starting the culture, so the third day counts as treatment day 1 (T1). The treatment was lasted for 4 days. (F) RNA was isolated from both wild type and SMAD4^{-/-} embryoid bodies at different time points, from day 0 (ES), 3 (EB3), 6 (EB6), 9 (EB9) and 12 (EB12).

Discussion

In the present study, we disrupted TGF- β /SMAD4 signaling in the visceral endoderm by crossing SMAD4 conditional mutant mice with mice carrying a *TTR-Cre* transgene. We illustrated that the *Smad4^{Co/Co};TTR-Cre* embryos displayed severe abnormalities in the development of anterior structures; however, they had relatively normal posterior structures. This is unlikely caused by a lack of Cre activity as Cre-mediated deletion of lac-Z reporter gene is detected in the entire visceral endoderm at early post-implantation stages. Rather, this finding suggests that TGF- β /SMAD4 signaling has a more critical role

in the AVE than it does in posterior visceral endoderm.

We also confirmed that the lethality of *Smad4^{Co/Co};TTR-Cre* embryos is indeed due to SMAD4 deficiency in the extraembryonic endoderm by aggregating *Smad4^{Co/Co};TTR-Cre* embryos with wild-type tetraploid embryos. It has been shown that tetraploid wild-type cells preferentially incorporate into visceral endoderm and extraembryonic endoderm but they cannot participate in embryonic development [37, 38], and therefore entire embryos are formed by *Smad4^{Co/Co};TTR-Cre* embryos. The fact that *Smad4^{Co/Co};TTR-Cre* tetraploid embryos survive through the gastrulation process provides strong

evidence that TGF- β /SMAD4 signaling in the visceral endoderm and extraembryonic tissue is critical for early post-implantation embryogenesis and normal patterning. Due to the fact that the expression of *TTR-Cre* is in the entire visceral endoderm (Fig. 1), the *TTR-Cre* transgenic mice should serve as an important tool for testing functions of genes in this tissue for their ability in regulating gene expression and embryonic patterning prior to and during gastrulation. Of note, a recent study also generated a *TTR-Cre* transgenic mouse line, which showed similar Cre activity by using R26R reporter line [44]. The *TTR* promoter used to drive Cre is known to have a similar expression pattern compared with the endogenous *TTR* gene in some adult organs such as liver, pancreas, gut, and gallbladder [44, 45]. *TTR-Cre* transgenic mice can also be used for studying gene function in these tissues.

The AVE provides nutrition and physical support to embryos, and also plays a critical role for mesoderm formation, and head induction and patterning [4-6, 33, 34, 46]. Many molecules, including members of TGF- β superfamily (Nodal, Lefty1), receptors (ActRIB, ActRIIA, ActRIIB), and intracellular mediators (Smad2, and Smad4) and those that are not directly related to TGF- β , such as Hex1, Lim1, HNF3 β , Cer1, Otx2, mDkk1, and Goosecoid, are expressed in the AVE [4, 6, 33, 34]. Embryos deficient for some of these genes exhibit phenotypes including failure to initiate gastrulation, mesoderm induction (ActRIB [12], ActRIIA and ActRIIB double mutants [13], Smad2 [47] and Smad4 [28, 29]), mesoderm patterning defects (Nodal [15], Hnf3- β [48]), L-R axis position defect (Lefty1 [49]), and anterior truncation (Otx2 [50], Lim1 [36]). However, the precise role of these molecules in embryonic patterning and their relationship in signaling cascades remain elusive.

We show here that the abnormal development of the *Smad4^{Co/Co};TTR-Cre* embryos is associated with significantly reduced or absence of expression of many genes important for early embryonic development. The absence of these genes could either serve as a causative reason or simply as a victim to the abnormal development in mutant embryos. To distinguish this, we studied early post-implantation embryos, and found that expression of *Lim1*, *Cer1* and *Hnf3 β* is already diminished in *Smad4^{Co/Co};TTR-Cre* embryos at stages prior to the onset of morphological abnormalities. This data suggests that the absence of expression of these genes is not secondary to the SMAD4 deficiency, rather it argues that their expression is positively regulated by SMAD4 signaling. This notion is confirmed by our *in vitro* study where the treatment of TGF- β induces expression of these genes

in embryoid bodies formed by wild type ES cells, but not by SMAD4^{-/-} ES cells. Thus, our study reveals a cascade of TGF- β /SMAD4 signaling in the AVE through regulating expression of some important genes, including *Cer1*, *Hnf3 β* , and *Lim1* that determine anterior embryonic patterning and head induction in mouse embryos.

In addition to the AVE, many members of TGF- β superfamily are expressed in the underlying epiblasts [4-7, 11, 16]. As a common mediator for TGF- β superfamily [8, 9], SMAD4 should mediate TGF- β signaling from both the AVE and epiblast. To investigate this, we have also deleted SMAD4 in the epiblast using *Mox2-Cre*. We found that many of the *Smad4^{Co/Co};Mox2-Cre* embryos developed into head-fold stages and exhibited relatively normal head process. Indeed, the SMAD4-deficient epiblast seems to be able to form most, if not all, mesoderm derivatives. Loss of SMAD4 in the epiblast also does not affect expression of genes that is severely affected in *Smad4^{Co/Co};TTR-Cre* embryos. A previous investigation also deleted SMAD4 in the epiblast using *Sox2-Cre* [30]. The *Sox2Cre;Smad4^{CA/N}* embryos exhibited profound failure to pattern derivatives of the anterior primitive streak [30], which is more severe than the *Smad4^{Co/Co};Mox2-Cre* embryos generated here perhaps due to slightly earlier expression of *Sox2-Cre* [40] than *Mox2-Cre* [39]. Despite this, the *Sox2Cre;Smad4^{CA/N}* embryos and the SMAD4^{-/-} embryos fused with wild-type tetraploid embryos [28] do not display defects in many well-characterized TGF- β regulated processes involved in mesoderm formation and patterning. These studies, together with our analysis of *Smad4^{Co/Co};Mox2-Cre* embryos (Fig. 6) indicate that SMAD4 signaling in the epiblasts is dispensable for mesoderm induction although it is critical for head patterning.

In summary, we have studied functions of SMAD4 in the visceral endoderm and epiblast using a Cre-LoxP mediated tissue specific gene knockout approach. In contrast to our previous finding that loss of SMAD4 in both germ layers blocked egg cylinder elongation and mesoderm induction [29], we showed that SMAD4 deficiency in the epiblast has no major impact in mesoderm induction although it results in abnormal mesoderm patterning during gastrulation. This data is consistent with a similar finding reported previously [28, 30]. Importantly, analyzing a novel mutant strain generated by deleting SMAD4 in the visceral endoderm, we uncovered an essential role of SMAD4 in the visceral endoderm that mediates TGF- β signaling and regulates expression of genes in the AVE, where they specify anterior embryonic patterning and head induction. These data indicate that

TGF- β /SMAD4 signaling has a distinct role in the visceral endoderm and underlying epiblast during gastrulation in mesoderm patterning and head induction, while joined signaling from both layers is critical for egg cylinder development and mesoderm induction, leading to the initiation of gastrulation.

Materials and Methods

Mice and genotyping analysis

The *Smad4^{Co/Co};TTR-Cre* mice and *Smad4^{Co/Co};Mox2-Cre* mice were generated by crossing the *Smad4^{Co/Co}* mice [32] with *TTR-Cre* transgenic mice (X.Y. Fu, manuscript in preparation), and *Mox2-Cre* transgenic mice [39], respectively. *Smad4* conditional mutant mice are genotyped by PCR using a pair of primers flanking one of the loxP sites: forward primer (5'-GACCCAAACGTCACCTTCAC-3') and reverse primer-1 (5'-GGGCAGCGTAGCATATAAGA-3'). This pair of primer amplifies a fragment of about 450 pb from wild type allele and a fragment of about 510 pb from *Smad4* conditional allele. After the Cre mediated recombination, the mutant *Smad4* allele is genotyped by using the forward primer and reverse primer-2 (5'-AAGAGCCACAGGTCAAGCAG-3'). The PCR product is about 500 bp. We used a pair of common Cre primers, Cre-1 (5'-CCT GTT TIG CAC GTT CAC CG-3') and Cre-2 (5'-ATG CTT CTG TCC GTT TGC CG-3') to genotype *TTR-Cre* and *Mox2-Cre*. Animals were handled in accordance with guidelines of the NIDDK Animal Care and Users Committee.

Generation of tetraploid embryos and rescue of SMAD4 mutant mice

Generation of tetraploid embryos was performed as described [37, 38]. Briefly, CD-1 females (Charles River) were mated with stud males and sacrificed at E1.5. Two-cell stage embryos were flushed out of oviducts and electrofused using cell fusion machine (CF-150 Hungary) to form one-cell stage tetraploids. *Smad4^{Co/Co}* female mice were mated with *Smad4^{+ /Co};TTR-Cre* males to produce diploid embryos with various genotypes, including *Smad4^{Co/Co};TTR-Cre*, *Smad4^{Co/Co}*, and *Smad4^{+ /Co};TTR-Cre*. Two tetraploids were co-cultured with one diploid embryo to aggregate overnight at 37°C. The blastocysts were then transferred to CD-1 foster mothers that were sacrificed at day 10.5–11.5 of pregnancy. Genotyping of embryos was performed as described above. As *Smad4^{Co/Co};TTR-Cre* embryos without fusion with tetraploid cells do not survive at these stages, any *Smad4^{Co/Co};TTR-Cre* embryos with normal appearance were considered as embryos that are completely rescued by tetraploid cells.

Whole-mount in situ hybridization

Whole-mount in situ hybridization was carried out as described [51]. Anti-sense RNA probes were synthesized using the DIG RNA Labeling Kit (Roche Diagnostics, Mannheim, Germany) according to the manufacturer's recommendations.

Histology

Tissue was fixed in 10% neutral-buffered formalin (Sigma) at 4°C overnight, dehydrated through a graded alcohol series, xylene and paraffin, and then embedded in paraffin. Sections of 5 mm were prepared for H&E and antibody staining using regular procedures.

Embryoid body differentiation and TGF- β treatment

Embryoid body differentiation was performed as described [52]. Briefly, 6X10⁶ cells were plated in 10-cm gelatin-coated dishes in the absence of feeder cells in ES cell medium. After 2 days in culture, small ES cell clumps were lifted off the plates by gentle trypsinization and transferred into suspension culture in ES cell medium without LIF in 10-cm bacteria plate. Cells were treated with 10ng/ml TGF- β 1 (R&D Systems) after 48 hours, harvest samples at different time points as indicated in figure 7 for analysis.

X-gal staining

Embryos were stained in X-gal overnight at 37°C as described [53]. Embryos were washed in PBS twice after staining, then fixed in 4% paraformaldehyde for one hour, dehydrated through a graded alcohol series, treated with xylene, and embedded in paraffin. Five μ m sections were prepared and counterstained with Harris hematoxylin according to standard procedures.

RT-PCR

Total RNA was extracted from cells using RNA STAT-60 (Tel-Test Inc.). RT was carried out using the Cell to cDNA kit from Ambion. RT-PCR was performed using the following primers for the genes of *Hnf1*, *Gata4*, *Nodal*, *EndoA*, *Hex*, *T*, and *Lim1*: *Hnf1*-F: 5'-GAA AGC AAC GGG AGA TCC TCC GAC-3', *Hnf1*-R: 5'-CCT CCT CCA CTA AGG CCT CCC TCT CTT CC-3'; *Gata4*-F: 5'-CAG CCC CTA CCC AGC CTA CAT-3', *Gata4*-R: 5'-GTG CCC CAG CCT TTT ACT TTG-3'; *Nodal*-F: 5'-CCC CAC AGG GTT AGG ACA CTC G-3', *Nodal*-R: 5'-TGC TGA AAG TGC TGT CTG TCT GCT C-3'; *EndoA*-F: 5'-TTC AGC AGC CGC TCG TTC AC-3', *EndoA*-R: 5'-TTC TCC TGA GTG CGC ACA GC-3'; *Hex*-F: 5'-GTT CTC CAA CGA CCA GAC CG-3', *Hex*-R: 5'-GGA GGG TGA ACA CTG CGA AC-3'; *T*-F: 5'-AGA AAG AAA CGA CCA

CAA AGA TG-3', T-R: 5'-ATT TAT TTA TTT TTC CCT TGT CC-3'; Lim1-2F: 5'-CCA AGC GAT CTG GTT CGC AG -3', Lim1-3R: 5'-GAT AAC ACG CAT GTT GAG GC - 3'; Gapdh-1: 5'-ACAGCCGCATCTTCTTGTGC-3'; Gapdh-2: 5'-TTTGATGTTAGTGGGGTCTCGC-3'.

Acknowledgment

We thank Dr. T Mak for providing *Smad4*^{-/-} ES cells, and members of Dr. Deng lab for their critical discussion of this work. This work was supported by the Intramural Research Program of the National Institute of Diabetes, Digestive and Kidney Diseases, National Institutes of Health, USA.

Conflict of Interests

The authors have declared that no conflict of interest exists.

References

- Nakaya Y, Sheng G. Epithelial to mesenchymal transition during gastrulation: an embryological view. *Dev Growth Differ.* 2008; 50: 755-766.
- Chenoweth JG, McKay RD, Tesar PJ. Epiblast stem cells contribute new insight into pluripotency and gastrulation. *Dev Growth Differ.* 2010; 52: 293-301.
- Arnold SJ, Robertson EJ. Making a commitment: cell lineage allocation and axis patterning in the early mouse embryo. *Nat Rev Mol Cell Biol.* 2009; 10: 91-103.
- Tam PP, Loebel DA, Tanaka SS. Building the mouse gastrula: signals, asymmetry and lineages. *Curr Opin Genet Dev.* 2006; 16: 419-425.
- Chea HK, Wright CV, Swalla BJ. Nodal signaling and the evolution of deuterostome gastrulation. *Dev Dyn.* 2005; 234: 269-278.
- Perea-Gomez A, Rhinn M, Ang SL. Role of the anterior visceral endoderm in restricting posterior signals in the mouse embryo. *Int J Dev Biol.* 2001; 45: 311-320.
- Weinstein M, Yang X, Deng C. Functions of mammalian smad genes as revealed by targeted gene disruption in mice [In Process Citation]. *Cytokine Growth Factor Rev.* 2000; 11: 49-58.
- Heldin CH, Miyazono K, ten Dijke P. TGF-beta signalling from cell membrane to nucleus through SMAD proteins. *Nature.* 1997; 390: 465-471.
- Massague J. TGF-beta signal transduction. *Ann Rev Biochem.* 1998; 67: 753-791.
- Weinstein M, Deng CX. Genetic disruptions within the murine genome reveal the numerous roles of the Smad gene family in development, disease, and cancer. In: Dijke PT and Heldin CH, eds. *Smad signal Transduction: Smads in proliferation, differentiation and disease.* US: Springer. 2006:151-171.
- Wu MY, Hill CS. Tgf-beta superfamily signaling in embryonic development and homeostasis. *Dev Cell.* 2009; 16: 329-343.
- Gu Z, Nomura M, Simpson BB, et al. The type I activin receptor ActRIB is required for egg cylinder organization and gastrulation in the mouse. *Genes Dev.* 1998; 12: 844-857.
- Song J, Oh SP, Schrewe H, et al. The type II activin receptors are essential for egg cylinder growth, gastrulation, and rostral head development in mice. *Dev Biol.* 1999; 213: 157-169.
- Winnier G, Blessing M, Labosky PA, et al. Bone morphogenetic protein-4 is required for mesoderm formation and patterning in the mouse. *Genes Dev.* 1995; 9: 2105-2116.
- Zhou X, Sasaki H, Lowe L, et al. Nodal is a novel TGF-beta-like gene expressed in the mouse node during gastrulation. *Nature.* 1993; 361: 543-547.
- Moustakas A, Heldin CH. The regulation of TGFbeta signal transduction. *Development.* 2009; 136: 3699-3714.
- Howe JR, Roth S, Ringold JC, et al. Mutations in the SMAD4/DPC4 gene in juvenile polyposis [see comments]. *Science.* 1998; 280: 1086-1088.
- Hahn SA, Hoque AT, Moskaluk CA, et al. Homozygous deletion map at 18q21.1 in pancreatic cancer. *Cancer Res.* 1996; 56: 490-494.
- Friedl W, Kruse R, Uhlhaas S, et al. Frequent 4-bp deletion in exon 9 of the SMAD4/MADH4 gene in familial juvenile polyposis patients. *Genes Chromosomes Cancer.* 1999; 25: 403-406.
- Li W, Qiao W, Chen L, et al. Squamous cell carcinoma and mammary abscess formation through squamous metaplasia in Smad4/Dpc4 conditional knockout mice. *Development.* 2003; 130: 6143-6153.
- Bornstein S, White R, Malkoski S, et al. Smad4 loss in mice causes spontaneous head and neck cancer with increased genomic instability and inflammation. *J Clin Invest.* 2009; 119: 3408-3419.
- Yang G, Yang X. Smad4-mediated TGF-beta signaling in tumorigenesis. *Int J Biol Sci.* 2010; 6: 1-8.
- Xu X, Ehdaie B, Ohara N, et al. Synergistic action of Smad4 and Pten in suppressing pancreatic ductal adenocarcinoma formation in mice. *Oncogene.* 2010; 29: 674-686.
- Xu X, Kobayashi S, Qiao W, et al. Induction of intrahepatic cholangiocellular carcinoma by liver specific disruption of Smad4 and Pten in mice. *Journal of Clinic Investigation.* 2006; in press
- Yang L, Mao C, Teng Y, et al. Targeted disruption of Smad4 in mouse epidermis results in failure of hair follicle cycling and formation of skin tumors. *Cancer Res.* 2005; 65: 8671-8678.
- Qiao W, Li AG, Owens P, et al. Hair follicle defects and squamous cell carcinoma formation in Smad4 conditional knockout mouse skin. *Oncogene.* 2006; 25: 207-217.
- Weinstein M, Monga SP, Liu Y, et al. Smad proteins and hepatocyte growth factor control parallel regulatory pathways that converge on beta1-integrin to promote normal liver development. *Mol Cell Biol.* 2001; 21: 5122-5131.
- Sirard C, de la Pompa JL, Elia A, et al. The tumor suppressor gene Smad4/Dpc4 is required for gastrulation and later for anterior development of the mouse embryo. *Genes Dev.* 1998; 12: 107-119.
- Yang X, Li C, Xu X, et al. The tumor suppressor SMAD4/DPC4 is essential for epiblast proliferation and mesoderm induction in mice. *Proc Natl Acad Sci U S A.* 1998; 95: 3667-3672.
- Chu GC, Dunn NR, Anderson DC, et al. Differential requirements for Smad4 in TGFbeta-dependent patterning of the early mouse embryo. *Development.* 2004; 131: 3501-3512.
- Soriano P. Generalized lacZ expression with the ROSA26 Cre reporter strain. *Nat Genet.* 1999; 21: 70-71.
- Yang X, Li C, Herrera PL, et al. Generation of Smad4/Dpc4 conditional knockout mice. *Genesis.* 2002; 32: 80-81.
- de Souza FS, Niehrs C. Anterior endoderm and head induction in early vertebrate embryos. *Cell Tissue Res.* 2000; 300: 207-217.
- Beddington RS, Robertson EJ. Axis development and early asymmetry in mammals. *Cell.* 1999; 96: 195-209.
- Shawlot W, Deng JM, Behringer RR. Expression of the mouse cerberus-related gene, *Cerr1*, suggests a role in anterior neural induction and somitogenesis. *Proc Natl Acad Sci U S A.* 1998; 95: 6198-6203.
- Shawlot W, Behringer RR. Requirement for *Lim1* in head-organizer function. *Nature.* 1995; 374: 425-430.

37. Nagy A, Gocza E, Diaz EM, *et al.* Embryonic stem cells alone are able to support fetal development in the mouse. *Development*. 1990; 110: 815-821.
38. Li C, Guo H, Xu X, *et al.* Fibroblast growth factor receptor 2 (Fgfr2) plays an important role in eyelid and skin formation and patterning. *Dev Dyn*. 2001; 222: 471-483.
39. Tallquist MD, Soriano P. Epiblast-restricted Cre expression in MORE mice: a tool to distinguish embryonic vs. extra-embryonic gene function. *Genesis*. 2000; 26: 113-115.
40. Hayashi S, Lewis P, Pevny L, *et al.* Efficient gene modulation in mouse epiblast using a Sox2Cre transgenic mouse strain. *Gene Expr Patterns*. 2002; 2: 93-97.
41. Thorey IS, Meneses JJ, Neznanov N, *et al.* Embryonic expression of human keratin 18 and K18-beta-galactosidase fusion genes in transgenic mice. *Dev Biol*. 1993; 160: 519-534.
42. Soudais C, Bielinska M, Heikinheimo M, *et al.* Targeted mutagenesis of the transcription factor GATA-4 gene in mouse embryonic stem cells disrupts visceral endoderm differentiation in vitro. *Development*. 1995; 121: 3877-3888.
43. Abe K, Niwa H, Iwase K, *et al.* Endoderm-specific gene expression in embryonic stem cells differentiated to embryoid bodies. *Exp Cell Res*. 1996; 229: 27-34.
44. Kwon GS, Hadjantonakis AK. Transthyretin mouse transgenes direct RFP expression or Cre-mediated recombination throughout the visceral endoderm. *Genesis*. 2009; 47: 447-455.
45. Costa RH, Van Dyke TA, Yan C, *et al.* Similarities in transthyretin gene expression and differences in transcription factors: liver and yolk sac compared to choroid plexus. *Proc Natl Acad Sci U S A*. 1990; 87: 6589-6593.
46. Srinivas S. The anterior visceral endoderm-turning heads. *Genesis*. 2006; 44: 565-572.
47. Weinstein M, Yang X, Li C, *et al.* Failure of egg cylinder elongation and mesoderm induction in mouse embryos lacking the tumor suppressor smad2. *Proc Natl Acad Sci U S A*. 1998; 95: 9378-9383.
48. Ang SL, Rossant J. HNF-3 beta is essential for node and notochord formation in mouse development. *Cell*. 1994; 78: 561-574.
49. Meno C, Shimono A, Saijoh Y, *et al.* lefty-1 is required for left-right determination as a regulator of lefty-2 and nodal. *Cell*. 1998; 94: 287-297.
50. Acampora D, Mazan S, Lallemand Y, *et al.* Forebrain and mid-brain regions are deleted in Otx2^{-/-} mutants due to a defective anterior neuroectoderm specification during gastrulation. *Development*. 1995; 121: 3279-3290.
51. Riddle RD, Johnson RL, Laufer E, *et al.* Sonic-hedgehog mediates the polarizing activity of the zpa. *Cell*. 1993; 75: 1401-1416.
52. Xiong JW, Battaglino R, Leahy A, *et al.* Large-scale screening for developmental genes in embryonic stem cells and embryoid bodies using retroviral entrapment vectors. *Dev Dyn*. 1998; 212: 181-197.
53. Mansour SL, Goddard JM, Capecchi MR. Mice homozygous for a targeted disruption of the proto-oncogene int-2 have developmental defects in the tail and inner ear. *Development*. 1993; 117: 13-28.